EXTERNAL CLUSTER COMBUSTION OF BINARY-FUEL DROPS

J. Bellan

Jet Propulsion Laboratory

California Institute of Technology

Pasadena CA 91109

Abstract

A model describing external sheet combustion of a cluster of drops has been developed for clusters of binary-fuel drops. The binary-fuel is assumed to be a solvent-solute combination in which the solute is much more volatile than the solvent. The initial solvent mass fraction within the mixture is larger than that of the solute. Both the ignition timing and location are calculated using previously derived criteria; for the range of air/fuel mass ratios considered, ignition always occurs around the cluster. Following ignition, an internal flash flame burns all the oxygen within the cluster. An external sheet flame ensues, fueled by vapor released from the cluster. Results show that drop interactions are important in modifying the amount of fuel burned. It is only for small initial cluster velocities and for large air/fuel mass ratios that the external flame behaves approximately like a classical diffusion flame in that it burns almost all the fuel released from the cluster. For all other conditions, the amount of fuel burned is

smaller than that released from the cluster. These conclusions are independent of the initial solute mass fraction and of the Arrhenius ignition parameters which are assumed identical for solvent and solute.

1 Introduction

Most fuels used in practical combustion liquid-fuel sprays devices are blends of several components. 111 many cases, the composition of the fuel is critical to the operation of the device since it affects efficiency and polluti on production. Consequently, a substantial number of studies (cf. review by Law ,1986) addressed the problem of single, isolated multicomponet drop evaporation, ignition and combustion. These studies have contributed important understanding of the physics of the internal drop processes and their coupling to the flow surrounding the drop. However, according to experimental evidence from Allen and Hanson (1986a, 1986b), Mao et al. (1985), McDonell et al. (1992), Mizutani et al. (1993) and Rudoff et al. (1989), sprays do not burn with individual drop flames; instead, there is a multitude of flames, with each flame surrounding a group of drops which is called here a cluster. These external cluster flames are an important indication of drop interactions.

These interactions and the consequences they have upon internal drop processes are studied here in the context of binary-fuel drops because binary-fuel are a practical representation of typical fuels often composed of tens of pure fuels. Since this study is done in the context of alternate fuels, the solvent represents the large mass fraction, viscous, nonvolatile components whereas the solute represents the much smaller mass fraction, low-viscosity, volatile components.

2 Description of the Model

'1'1 ic conf iguration studied is that of a spherical cluster of relatively cold spherical drops exposed to an axial flow at a higher temperature as depicted in Fig. 1 in Bellan and Harstad (1990). Inside the cluster, the drops move radially with respect to the cluster center and the relative radial motion of the drops with respect to the gas is assumed to be self-similar (Harstad and 1 3ellan, 1 989). The mathematical model is based upon the formulations of: (i) Harstad and Bellan (199]) for evaporation of binary-fuel drops in clusters, (ii) Bellan and Harstad (in print.) for ignition of binary-fuel drops in clusters, and (iii) Bellan and Harstad (1 W()) for single-component fuel cluster-combustion, adapted here for binary-fuel drops. The internal-cluster flash flame equations and the external-cluster equations for binary-fuel combustion are similar to those for single-component fuel.

Ignition may be initiated by either solvent or solute according to the 1)amköhler number criterion described in Bellan and Harstad (in print) under the assumption that the ignition chemistries of the two components are independent. The internal flash flame following ignition (Bellan and Harstad, 1 990) burns all of the oxygen inside the cluster; the oxygen is apportioned between solvent and solute according to their average mass fractions at ignition. F'ollowing the flash f] ame, a flame surrounds the cluster, similar to those observed experimentally; the model is based on the assumption that this flame is infinitesimally thin. The general location of the flame (individual, collective or intermediary internal cluster flame) is calculated at ignition according to a criterion already used in I 3ellan and 1 Iarstad (1987); for the situations studied here, calculations show that the flame is always of the collective type. The location of the flame during collective burning is calculated from the conservation equations in the following.

2.1 Conservation equations for the internal flash flame

These conservation equations are global and describe the internal cluster flame prior to the establishment of the external cluster flame. Similar to Bellan and Harstad (1990), the total nondimensional amount of gas mass and air in the cluster before ignition are defined as

$$\widehat{M}_g = \frac{1}{Nm_d^0}\left[N\int_R \rho_g 4\pi r^2 dr + (V - \frac{4\pi a^3 N}{3})\rho_{ga}\right] \quad (1)$$

$$\widehat{M}_{air} = \frac{1}{Nm_d^0}\left[N\int_R^a \rho_g(1 - Y_{F,V} - Y_{F,S})4\pi r^2 dr + (V - \frac{4\pi a^3 N}{3})\rho_{ga}(1 - Y_{F,V,a} - Y_{F,S,a})\right] \quad (2)$$

and the total nondimensional sensible enthalpy is defined as

$$\widehat{H}_g = \frac{1}{Nm_d^0}\left[N\int_R^a \rho_g C_{pg}(\theta_g - \theta_{ref})4\pi r^2 dr + (V - \frac{4\pi a^3 N}{3})\rho_{ga}C_{pg}(\theta_{ga} - \theta_{ref})\right] \quad (3)$$

The cluster contains only fuel and air so that

$$\widehat{M}_{Fv} = \widehat{M}_g - \widehat{M}_{air}. \quad (4)$$

The total amount of fuel mass burned is in stoichiometric proportion with O_2 burned and since internal burning stops only when all internal O_2 disappears

$$\widehat{M}_{F,B} = \widehat{M}_{F,V} + \widehat{M}_{F,S} = \widehat{M}_{O_2}/(\Phi'_{s,V} + \Phi'_{s,S}) \quad (5)$$

In order to maintain the same temperature profile within the drops, combustion is assumed to occur at fixed effective latent heat. Thus, the eight dependent variables determining the post-ignition st ate of the cluster, $\theta^*_{ga}, \theta^*_{gs}, Y^*_{F,V,a}, Y^*_{F,S,a}, Y^*_{F,V,s}, Y^*_{F,S,s}, a^*$, and C^* are the solution of the following global conservation equations:

$$\widehat{M}^*_{F,V} = \widehat{M}_{F,V} - \widehat{M}_{F,V,B} \quad (6)$$

$$\widehat{M}^*_{F,S} = \widehat{M}_{F,S} - \widehat{M}_{F,S,B} \tag{7}$$

$$\widehat{M}^*_g = \widehat{M}_g \tag{8}$$

$$\widehat{H}^*_g = \widehat{H}_g + H_{c,V}\widehat{M}_{F,V,B} + H_{c,S}\widehat{M}_{F,S,B} \tag{9}$$

$$Y^*_{F,i,s} = 1 + (Y^*_{F,i,a} - 1)\exp[C^* Z(R^*_1)] \tag{10}$$

$$Z(R^*_1) = R^*_1(\theta^\infty_g)^{0.65}\int_{R^*_1}^{R^*_2}\frac{dy}{y^2\theta_g^{0.65}} \tag{11}$$

$$C^* = \frac{1}{Z(R^*_1)}\ln\{1 + \frac{L}{L_{bn}}\frac{\theta^*_{ga} - \theta^*_{gs}}{\frac{R^*_1}{C^*}\frac{\lambda_l}{C_{pg}(\rho_g D)^\infty}\frac{\partial\theta^*_l}{\partial z}\Big|_{z=1}}\} \tag{12}$$

$$C^* = -\alpha(R^*_1)^2\frac{R^0}{4\pi(\rho_g D)^\infty}\{1atm\exp[\frac{C_{pg}w_F}{R_u}(\frac{1}{\theta_{bn}} - \frac{1}{\theta^*_{gs}}) + \frac{w_F\triangle C_p}{R_u}(1 \quad \frac{\theta_{bn}}{\theta^*_{9.?}} + \ln\frac{\theta_{bn}}{\theta^*_{gs}}\Big)1$$

$$- \quad p^\infty(\frac{\theta^*_l}{\theta^*_{gs}})^{0.5}\frac{Y^*_{F,S,s}}{Y^*_{F,S,s}+\frac{w_F}{w_{ag}}(1 - Y^*_{F,S,s})}(\frac{w_F C_{pg}}{2\pi R_u L_{bn}\theta^*_{ngs}})^{0,,5} \tag{13}$$

where $i = V$ or $i = S$ in Eq. 10. In Eq. 13 it has been assumed that the evaporation rate is controlled by the solvent [because ignition occurs late in the drop lifetime, when the slip velocity is very small as shown in Bellan and Harstad, (in print)], and thus L, L_{bn}, θ_{bn} and w_F appearing in Eqs. 12 and 13 are those of the solvent. In Eq. 13 $C_{pg} = C_{p,air} + C_{p,V}Y_{F,V} + C_{p,S}Y_{F,S}$ and appears because of nondimensionalization.

Because of temperature continuity at the drop surface, $\theta^*_l = \theta^*_{gs}$; the solution for $\theta_l(z)$ is obtained as in Bellan and Harstad (1987b). The solution of Eqs. 6-13 provide the initial conditions for the external cluster flame equations.

2.2 Conservation equations for the external cluster flame

The external cluster flame equations are adapted from Bellan and Harstad (1990) with

$$\dot{M}_F = 4\pi \tilde{R}_{cl}^2 \rho_{ga} (Y_{F,V,a} + Y_{F,S,a}) u_{re} \tag{14}$$

where $u_{re} = d\tilde{R}_{cl}/dt - u_{ge}$ is the relative velocity of the gas with respect to the cluster boundary. u_{ge}, the gas radial velocity at the cluster boundary, is calculated assuming that the relative radial motion for an internal drop is self-similar as in Harstad and Bellan (1989), except that here there are no electrostatic effects; the drop momentum is changed by forces resulting for drop evaporation, drop drag and cluster drag as an entity. The total mass release rate from the cluster is

$$\dot{M} = N\dot{m}_{loss} = 4\pi \tilde{R}_{cl}^2 \rho_{ga} u_{re} \tag{15}$$

and the cluster behaves as a mass source for the flame.

2.2,1 solution for $\tilde{R}_{cl} < \tilde{r} < \tilde{R}_f$

The quasi-steady conservation convection-diffusion equations with variable $\rho_g D$ have similarity solutions

$$\Gamma(\tilde{y}) = C_1 + C_2 \exp[\tilde{C}(\rho_g D)^{\infty} \int_{\tilde{y}_{cl}}^{\tilde{y}} \frac{d\tilde{y}}{\tilde{y}^2 \rho_g D}] \tag{16}$$

where Γ stands for $\theta_g, Y_{F,V}$, or $Y_{F,S}$, $\tilde{y} = \tilde{r}/R^0, \tilde{y}_{cl} = \tilde{R}_{cl}/R^0$ and

$$\tilde{C} = -\frac{\dot{M}}{4\pi R^0 (\rho_g D)^{\infty}} \tag{17}$$

Constants c_1 and c_2 are calculated from boundary conditions at $\tilde{R}_{cl}$ and $\tilde{R}_f$ assuming that the fuel is entirely consumed at the flame:

$$C_{1\theta} = [\theta_{ga} \exp(B) - \theta_f]/[\exp(B) - 1], \; C_{2\theta} = (\theta_f - \theta_{ga})/[\exp(B) - 1] \tag{18}$$

$$C_{1i} = -[Y_{F,i,a}\exp(B)]/[1-\exp(B)],\ C_{2i} = Y_{F,i,a}/[1-\exp(B)] \tag{19}$$

$$B \equiv \tilde{C}(\rho_g D)^{\infty}\int_{\tilde{y}_{cl}}^{\tilde{y}_f}\frac{d\tilde{y}}{\tilde{y}^2\rho_g D} \tag{20}$$

where $\tilde{y}_f \equiv \tilde{R}_f/R^0$, and $i = V$ or $i = S$.

2.2.2 Solution for $\tilde{R}_f^+ < \tilde{r} < \tilde{R}_{eff}^{\infty}$

The quasi-steady convection-diffusion equations with variable $\rho_g D$ have similarity solutions

$$\Gamma(\tilde{y}) = D_1 + D_2\exp[\tilde{C}(\rho_g D)^{\infty}\int_{\tilde{y}}^{\tilde{y}_{eff}^{\infty}}\frac{d\tilde{y}}{\tilde{y}^2\rho_g D}] \tag{21}$$

where Γ stands for $\theta_g$or Y_{o_2}. Constants D_1 and D_2 are calculated from boundary conditions at $\tilde{R}_f$ and the effective distance from the cluster center to the surroundings, $\tilde{R}_{eff}^{\infty}$.

$$D_{1\theta} = [\theta_{g\infty}\exp(G) - \theta_f]/[\exp(G) - 1],\ D_{2\theta} = (\theta_f - \theta_g^{\infty})/[\exp(G) - 1] \tag{22}$$

$$D_{1O_2} = -[Y_{o_2}^{\infty}\exp(G)]/[1-\exp(G)],\ D_{2O_2} = Y_{o_2}^{\infty}/[1-\exp(G)] \tag{23}$$

$$G \equiv \tilde{C}(\rho_g D)^{\infty}\int_{\tilde{y}_f}^{\tilde{y}_{eff}^{\infty}}\frac{d\tilde{y}}{\tilde{y}^2\rho_g D} \tag{24}$$

and $\tilde{y}_{eff}^{\infty} = \tilde{R}_{eff}^{\infty}/R^0$. $\tilde{y}_{eff}^{\infty}$ is calculated from the equality of the time-integrated fuel mass released from the cluster prior to ignition, to the field-integral of the fuel mass in the cluster surroundings at ignition

$$\int_0^{t_{ign}}\dot{M}_F = 4\pi\,(R^0)^3\int_{\tilde{y}_{cl}}^{\tilde{y}_{eff}^{\infty}}\rho_g(\quad\rho_g\,Y_{F,V}^{bi} + Y_{F,S}^{bi})\tilde{y}^2 d\tilde{y}. \tag{25}$$

The fuel mass in the cluster surroundings is given by the quasi-steady solution just before ignition

$$Y_{F,i}^{bi}(\tilde{y}) = \frac{Y_{F,i,a}}{1-\exp(K)}\{-\exp(K) + \exp[\tilde{C}(\rho_g D)^{\infty}\int_{\tilde{y}_{cl}}^{\tilde{y}}\frac{d\tilde{y}}{\tilde{y}^2\rho_g D}]\} \tag{26}$$

$$K \equiv \tilde{C}(\rho_g D)^{\infty}\int_{\tilde{y}_{cl}}^{\tilde{y}_{eff}^{\infty}}\frac{d\tilde{y}}{\tilde{y}^2\rho_g D} \tag{27}$$

for $i = V$ or $i = S$ under the assumption that $Y_{F,i}(\widetilde{y}^{\infty}_{eff}) \approx 0$. It is assumed that $\widetilde{y}^{\infty}_{eff}$ remains constant after ignition since the dense clusters studied here tend to ignite rather late in their lifetime.

2.2.3 Calculation of flame mass consumption rate, θ_f and $\widetilde{R}_f$.

Mass consumption rate The fuel consumption rate at the flame surface is

$$\dot{M}_c = \dot{M}_F - 4\pi(R^0)^3 \frac{d}{dt}\int_{\widetilde{y}_{cl}}^{\widetilde{y}_f} \widetilde{y}^2 \rho_g (Y_{F,V} + Y_{F,S}) d\widetilde{y} \tag{28}$$

which is not constrained to equal $\dot{M}$, as it is in the classical isolated drop theory, both because N_2 escapes the cluster together with fuel and because the flame position may change. In terms of a nondimensional time τ and a nondimensional density $\widehat{\rho}_g$, Eq. 28 becomes

$$\widetilde{C}_c = \widetilde{C}_F - \frac{d}{d\tau}\int_{\widetilde{y}_{cl}}^{\widetilde{y}_f} \widetilde{y}^2 \widehat{\rho}_g (Y_{F,V} + Y_{F,S}) d\widetilde{y}. \tag{29}$$

Flame position, $\widetilde{R}_f$ The condition that the fluxes of fuel and O_2 must be in stoichiometric proportion at the flame surface yields an integral equation for $\widetilde{y}_f$

$$\frac{\exp(-B) - 1}{\exp(-G) - 1} = -\frac{Y_{F,V}\Phi'_{s,V} + Y_{F,S}\Phi'_{s,S}}{Y^{\infty}_{O_2}} \tag{30}$$

under the assumption that $Y_{O_2}, Y_{F,V}, Y_{F,S}$ are null at the flame surface.

Flame temperature, θ_f The continuity of heat fluxes through the flame is

$$\dot{M}C_{pg}T_f - 4\pi\widetilde{R}_f^2\lambda_g\frac{dT_g}{d\widetilde{r}}\Big|_{\widetilde{R}_f^-} + \dot{M}_c H_c = \dot{M}C_{pg}T_f - 4\pi\widetilde{R}_f^2\lambda_g\frac{dT_g}{d\widetilde{r}}\Big|_{\widetilde{R}_f^+} \tag{31}$$

where $H_c = H_{c,V}Y_{F,V} + H_{c,S}Y_{F,S}$. Equation 31 is nondimensionalized and solved for θ_f by using Eq. 30 and the solutions for θ_g on both sides of the flame. This yields

$$\theta_f = \frac{Y_{O_2}^{\infty}(\theta_{ga} + H_c/L_{bl}) + \theta_g^{\infty}(Y_{F,HV}\Phi'_{s,V} + Y_{F,S}\Phi'_{s,S})}{Y_{O_2}^{\infty} + Y_{F,HV}\Phi'_{s,V} + Y_{F,S}\Phi'_{s,S}} \tag{32}$$

3 Method of Solution

The initial conditions specify Φ^0; R^0; u_{cl}^0; $Y_{V,l}^0$; T_{ga}^0 which is assumed to be the same as the surrounding-cluster gas temperature; the interstitial initial composition of the cluster gas which is assumed to be identical to that of the gas surrounding the cluster; the initial uniform drop temperature, T_s^0; $\widetilde{R}_{cl}^0$; E_{ign}; A_{ign}; $p = 1$ atm; and the thermophysical and thermochemical properties of the fuels. $E_{ign}$and A_{ign}, used in the Damköhler number criterion for ignition are assumed identical for solvent and solute.

Evaporation and drop motion is calculated following Harstad and Bellan (1991) and at each time step the Damköhler number criterion for ignition is checked according to the model of Bellan and Harstad (in print). If ignition occurs, the conservation equations for the internal cluster flash flame are solved to yield the initial values for the external cluster flame and $\widetilde{y}_{eff}^{\infty}$. Calculations then proceed as follows: At each time step $\widetilde{y}_{cl}, \theta_{ga}, Y_{F,V,a}, Y_{F,S,a}, B$ and G are calculated using the model of Harstad and Bellan (1991) [the boundary conditions at the cluster surface are described in Bellan and Harstad (1988) in the formulation called 'strong turbulence' (model 2)]. Equations 29, 30 and 32 are then used to calculate $\theta_f, \widetilde{y}_f$ and $\widetilde{C}_c$, and due to strong nonlinearities the solution is iterated to convergence. Inherent in the utilization of the turbulent transfer model at the cluster surface is the assumption that the turbulent boundary layer thickness around the cluster is much smaller

than the distance from the cluster surface to the flame.

The calculation stops when the drop radius is 5% of the initial radius.

4 Discussion of Results

4.] General behavior

One conclusion from previous results for single-component clusters of drops [Bellan and Harstad *(1990)]* is that cluster flames exist only in a restricted range of air/fuel mass ratios, Φ's. If Φ is Very small, the cluster Inay be so dense that the drops extract {too much heat from the gas during evaporation, before heat transfer from the cluster surroundings may replenish it, and thus the temperature becomes too low to initiate ignition. For these clusters, evaporation proceeds without ignition until the drops disappear. Ignition might occur later in the gas phase, but this situation is outside the focus of this study. If Φ is very large at ignition, the gaseous mixture inside the cluster is fuel-lean and internal cluster combustion (Bellan and Harstad, 1990) depletes all gaseous fuel inside the cluster. With no gaseous fuel left to escape the cluster, the external cluster flame cannot become established. These two situations represent the lower and upper limits for the existence of cluster flames. Thus, cluster flames exist for clusters which arc not too dense (so that cluster ignition may occur) and for which the gaseous mixture is fuel-rich at, ignition.

During evaporation, the composition of the gas inside the cluster is determined by the evaporation of the two fuels and by the transport of fuel across the moving cluster boundary. Heat transfer from the cluster surroundings raises the cluster gas temperature thus inducing cluster expansion and engulfing the surrounding cluster gas; drop heating decreases the cluster gas temperature thus

inducing cluster contraction . The competition between these two processes determines the motion of the cluster boundary, the cluster gas composition and its temperature.

Solvent and solute evaporate from the drop at rates determined by the internal drop and drop-surface processes as explained elsewhere (Harstad and Bellan, 1991). These processes depend upon the relative velocity between drops and gas which is the solution of the momentum equations. If the relative velocity at the drop surface, u_{sl}, is negligible so that there is no shear and therefore no induced circulatory motion inside the drop, the solute evaporates at the same rate as the solvent; this has been called 'surface layer stripping' (Harstad and Bellan, 199). In Contrast, if the relative velocity at the drop surface is strong enough to induce circulation nside the drop, liquid mass diffusion becomes an important process and preferentially enhances evaporation of the solute; this causes the solute mass fraction to decrease inside the drop. The relative importance of liquid mass diffusion and surface layer stripping is quantified by a number $Bc \equiv -[R/(D_m u_l)]^{0.5} dR/dt$ (Harstad and Bellan, 1991) where u_l is the liquid circulatory velocity inside the drop. If $Bc << 1$, liquid mass diffusion controls solute evaporation whereas if $Bc >> 1$, surface layer stripping controls solute evaporation. As shown in Harstad and Bellan (1991), u_l is a function of u_{sl}.

4.2 1 'arametric study

The situations studied arc all identified n '1'able 1 anc the symbols correspond to those in the figures. The cluster gas is initially at rest but as the drops I11OVC, they entrain the gas which eventually acquires a velocity of its own. In all calculations $T_{ga}^0 = 1300$ K, $p = 1$ atm, $T_{gs}^0 = 350$ K, $R^0 = 2 \times 10\text{-}3$ cm, $\tilde{R}_{cl}^0 = 3$ cm and $Y_{F,V,a}^0 = Y_{F,S,a}^0 = o$.

Figures 1 and *2* display the fractions of solvent and of solute burned in the internal flash flame

and Fig. 3 displays their ratio, $f_{flash,V}/f_{flash,S}$. The fractions are increasing functions of Φ^0 because although for larger Φ^0's ignition occurs earlier in the drop lifetime, there is more O_2 inside the cluster and thus more of the fuel can burn. $f_{flash,V}/f_{flash,S}$ is always smaller than $Y^0_{V,l}/(1 - Y^0_{V,l})$ despite the initially larger relative velocity at the drop surface which preferentially evaporates the solute (this is the $Be \ll 1$ regime). This is explained by the eventual relaxation of u_{sl} (due to drag effects) well before ignition. The $Be \ll 1$ regime during which $Y_{V,l}$.has decreased is then followed by the $Be \gg 1$ regime. Then the preferential evaporation of the solute ceases and the solute evaporates at the rate of the solvent, that is at the frozen rate of the mass fraction when Be became $\gg 1$. This physical picture is the result of examining Be and the fractional evaporation rate of the solute, $\dot{m}_V/\dot{m}$, versus the residual drop radius, R_1. Additionally, this is confirmed by results showing that $f_{flash,V}/f_{flash,S}$ is a decreasing function of u^0_{cl} . This ratio increases with $Y^0_{V,l}$, has a negligible dependence upon the solvent identity and is independent upon the solute identity. The fact that this ratio is always smaller than $Y^0_{V,l}/(1 - Y^0_{V,l})$ indicates that eventually there is a steady-state situation that establishes where the amount of fuel escaping through the cluster boundary balances that evaporating from the drops. The ratio of the fractions appears to be constant with Φ^0.

Depicted in Figs. 4 and 5 are plots of the respective ratios (all at $R_1 = 0.05$) of the burned fraction during external cluster combustion to the fraction that escaped the cluster for solvent, $f_{b,S}/f_{loss,S}$, and for solute, $f_{b,V}/f_{loss,V}$. 'These plots show two types of behavior. Strong flames that are established further away from the cluster surface are encountered for smaller Φ^0's and for larger u^0_{cl}'s; Fig.6 displays the nondimensional distance from the flame to the cluster at $R_1 = 0.05$, and Snows that, this distance is insensitive to R_1 and depends only upon the initial conditions. In strong flames, only a small fraction of the fuel released from the cluster is burned by the time the drops disappear. For large u^0_{cl}'s, the small evaporation rate at the end of the drop lifetime can no longer

sustain the strong flame and instead of burning, extinction occurs. Mathematically, extinction is identified when the integrated consumption rate! at the flame decreases instead of increasing with time. This means that a quasi-steady flame can no longer be maintained although it is possible that an unsteady flame could still exist under these conditions. Weak flames are established very close to the cluster surface and they occur mainly for large Φ^0's and small u_{cl}^0 's. '1'1 rese flames behave asymptotically like classical quasi-steady diffusion flames where the fuel emitted by the cluster is almost entirely burned in the flame ($f_{b,S}/f_{loss,S}$ and $f_{b,V}/f_{loss,V}$ are nearly 1). For intermediary va] ues of u_{cl}^0, the classical behavior of the diffusion flame is never reached, indicating the importance of convective effects. Generally $f_{b,V}/f_{loss,V} \geq f_{b,S}/f_{loss,S}$, with the equality occurring only for weak diffusion flames because preferential evaporation of the solute is then unimportant. Examination of $f_{loss,V}/f_{loss,S}$ shows that it is only a very slightly increasing function of Φ^0 and depends mainly 11])011 $Y_{V,l}^0$ and u_{cl}^0. This ratio depends only slightly upon solvent identity and dots not depend upon solu te identity. A similar comment applies to $f_{b,V}/f_{b,S}$, except that instead of it being a slightl y increasing function of $\Phi 0$ it is a slightly decreasing function of Φ^0. Thus, although proportionally less solute is released from the cluster for small Φ^0, proportionally a larger fraction of solute is burned. The situation WI iere extinction is obtained represents an exception, as both ratios arc increasing functions of Φ^0.

For diffusion-dominated combustion, the fraction of fuel burned during external cluster combustion is an increasing function of Φ^0 (scc Fig. 7) because ignition occurs earlier during the drop lifetime. As convective effects become important, the! flame is relatively stronger in the small Φ^0 regime than in the purely diffusion regime as evidenced by the slope of the! nondimensional flame d istance to the cluster surface; as a result, it, burns a larger fraction of fuel. '1 'hus, for intermediary convective combustion, the fuel fraction burned during combustion is a nonmonotonic function of

Φ^0) and convex. When convection dominates, the flame is considerably stronger for small Φ^0's and accordingly an increasing fuel fraction is burned. The total fraction of fuel burned (flash flame and external combustion) is an increasing function of Φ^0 (see Fig.8) since the later ignition for small Φ^0's also corresponds to situations where there is less 0_2 inside the cluster and thus less fuel may be consumed by the flash flame.

Changing the ignition kinetics translates and enlarges or shrinks the collective flame regime on the Φ^0 axis but does not change qualitatively the results.

5 Summary and Conclusions

A model of binary-fuel drop-cluster combustion with external flame has been formulated This regime is not encountered for clusters that are dense enough to ignite after the drops are otally evaj mated, or for clusters that are so dilute as to have a lean gas phase at ignition. The external cluster flame range of air/fuel mass ratios corresponds to the dense and moderately dense cluster regimes.

Results show that even in the dense and moderately dense regimes (as distinct from the very dense cluster regime), drop interactions are important in modifying the fraction of fuel burned. For small initial cluster velocities and for large air/fuel mass ratios, external cluster flames tend to behave asymptotically as classical diffusion flames in that rate of combustion is asymptotically equal to that Of fuel released from the cluster. For small air/fuel mass ratios, the classical diffusion flame behavior is never encountered, independently of the initial cluster velocity, and the fraction of fuel bill'll(!d is always considerably smaller than the fraction Of fuel released from the cluster. For convective-dominated evaporation or for diffusive-convective evaporation, the classical diffusion

flame behavior is not encountered either. These results are independent of fuel composition or the initial mass fraction of solute within the fuel under the assumptions of much larger volatility and smaller initial mass fraction of the solute with respect to the solvent. '1'11(?s(! resultsare also independent of the ignition Arrhenius parameters providing that they are the same for solvent and solute.

ACKNOWLEDGMENT

The research described here was performed by the Jet 'ropulsion 1 aboratory, California Institute Of Technology, and was S11] ported by the US 1 Department Of Energy, Office of 1 ndustrial Technologies with Dr. Gideon Varga as technical monitor and Mr. R. Balthazar (Reimbursable and Energy Technologies Division, Albuquerque Operations) as administrative manager, through an agreement with the National Aeronautics and Space Administration. The equations coding and the many valuable discussions with Dr. K.G. Harstad are gratefully acknowledged.

REFERENCES

Allen, M. G. and Hanson, R. K., "Digital imaging of Species Concentration Fields in Spray Flames", 21st, Symp.(Int.) on Combustion, 1755-1762, 1 986a

Allen, 'M'." G. and Hanson, R. K., "Planar l aser-Induced-Flurescence Monitoring of OH in a spray Flame", Optical Engineering, 25, 12, 1309-1311, 1986b

Bellan, J. and Harstad, K., "Ignition of Non-Dilute Clusters of Drops in Convective flows", Combust. Sci. Technol., 53, 75-87, 1987a

Bellan, J. and Harstad, K., '(Analysis of the Convective Evaporation of Nondilute Clusters of l)l'0])s", Int. J. Heat Mass Transfer, 30, 1, 125-136, 1987b

Bellan, J. and Harstad, K., Int. J. Heat Mass Transfer, 31, 8, 1655-1668, 1988

Bellan, J. and Harstad, K., "Evaporation, Ignition and Combustion of Non 1 Dilute Clusters of' 1 Drops", Combust. and l~'l.tune, 79, 272-286, 1990

Bellan, J. and Harstad, K., "Ignition of a I jirlary-fuel (Solvent-Solute) Cluster of 1 Drops", in print in Combustion Science and Technology

Harstad, K. and Bellan, J., "Electrostatic Dispersion of 1 Drops in Clusters", Combust. Sci. Technol., 63, 169-181, 1989

Harstad, K. and Bellan, J., "A Model of the Evaporation of Binary-Fuel Clusters of Drops", Atomization and Sprays, 1,367-388, 1991

Law, C. K., "Recent Advances in Multicomponnet Droplet Vaporization", paper 86-WA/HT-14 presented at the Winter Annual Meeting ASME

Mao, C-P., Oechsle, V. and Chigier, N. A., paper presented at, the Central/Western States Section Meeting/The Combustion Institute, San Antonio, Texas, 1985

McDonell, V. G., Adachi, M. and Samuelsen, G. S., "Structure of Reacting and Non-Reacting Swirling Air-Assisted Sprays", Combust. Sci. Technol., 82, 225-248, 1992

Mizutani, Y., Nakabe, K. Fuchihata, M. Akamatsu, P'., Zaizen, M. and El-Emam, S. H., Atomization and Sprays, 3, 125-135, 1993

Rudoff, R. C., Brena de la Rosa, A., Sankar, S. V. and Bachalo, W. D., "Time Analysis of Polydisperse Sprays in Complex Turbulent Environments", paper AI AA-89-0052, 27th Aerospace Sciences Meeting, Reno, Nevada, 1989

	solvent	solute	$u_{cl}^0, cm/s$	$Y_{V,l}^0$	$E_{ign}, kcal/mole$
-{	n-decane	n-hexane	20	0.2	30'
u	n-decane	n-hexane	80	0.2	30
$\vee$	n-decane	n-hexane	200	0.2	30
O	No.2GT	n-hexane	20	0.2	30
D	*NO.2GT*	n-decane	20	0.2	30
$\triangle$	*NO.2GT*	n-decar1(!	20	0.3	30
$\bigcirc$	n-decane	n-hexane	20	0.2	28.5

Table 1: Initial conditions for the parametric study

NOMENCLATURE

a radius of the sphere of influence
A preexponential constant in the Arrhenius law
B defined by Eq. 2 (I
C $-\dot{m}/[4\pi(\rho_g D)^{\infty} R^0]$
$\widehat{C}$ defined by Eq.17
$\widehat{C}_c$ $-\dot{M}_c/[4\pi(\rho_g D)^{\infty} R^0]$
$\widehat{C}_F$ $-\dot{M}_F/[4\pi(\rho_g D)^{\infty} R^0]$
C_i constants of integration
C_p specific heat at constant pressure
D gas diffusivity
D_i constants of integration
D_m liquid mass diffusivity
E activation energy in the Arrhenius law
f fuel fraction measured with respect to the initial mass
G defined by Eq. 24
H enthalpy
$\widehat{H}$ nondimensional enthalpy
L latent heat
$\dot{m}$ drop evaporation rate
$\dot{M}$ total net flux of mass released by the cluster
$\widehat{M}$ nondimensional mass
$\dot{M}_c$ fuel mass consumption rate at the flame surface:
$\dot{M}_F$ fuel mass rate released from cluster
N number of drops
p pressure
r radial coordinate originating at the drop center
$\hat{r}$ radial coordinate originating at the cluster center
R drop radius
$\widehat{R}$ radial dimensions associated with $\hat{r}$
R_1 R/R^0
R_2 a/R^0

R_u universal gas constant
t time
T temperature
u velocity
V cluster volume
w_i molecular weight of species i
$\widetilde{y}$ $\widetilde{r}/R^0$
Y_i mass fraction of species i
z r/R
Z defined by Eq. 11

Subscriptts

a at the edge of the sphere of influence; interstitial va] uc
ag ambient, gas
air refers to air
b burned in the external flame
bn normal boiling point
B burned in the internal flash flame
c consumption
cl cluster
f flame
$flash$ refers to the internal flash flame
F fuel
g gas
gc gas radial motion at the cluster edge
ign ignition
l liquid
$loss$ released by the cluster
$outer$ refers to the external flai ne
rc radial component at, cluster edge
s at surface
sl slip
S solvent
tot total (flash and outer)
V volatile (solute)

Superscripts

$*$ values after internal flash burning
0 initial conditions
at the in ner edge of the flai ne surface
+ at the outer edge of the flame Sill'face
bi before igni tion

Greek symbols

α	evaporation accomodation coefficient, taken to be uni ty
$\wedge C_p$	C_{pl} - C_{pg}
θ	$C_{pg}T'/L_{bn}$
λ	thermal conductivity
ρ	density
$\widehat{\rho}$	ρ_g/ρ_g^{∞}
τ	$tD^0/(R^0)^2$
Φ	air/fuel mass ratio
Φ_s	stoichiometric air/fuel mass ratio
Φ_s'	stoichiometric oxygen/fllcl mass ratio

FIGURE CAPTIONS

Figure 1 Solvent flash-flame burned fraction versus air/fuel mass ratio at a residual drop radius of 5%. Symbols are defined in 'Table 1.

Figure 2 Solute flash-flame burned fraction versus air/fuel mass ratio at a residual drop radius of 5%. Symbols are defined in 'Table 1.

Figure 3 Ratio of the flash-flame burned fractions versus air/fuel mass ratio at a residual drop radius of 5%. Symbols are defined in 'Table 1.

Figure 4 Ratio of solvent burned fraction in the external cluster flame! to released solvent fraction from the cluster versus air/fuel mass ratio at a residual drop radius of 5%. Symbols are defined in Table 1.

Figure 5 Ratio of solute burned fraction in the external cluster flame to released solute fraction from the cluster versus air/fuel mass ratio at a residual drop radius of 5%. Symbols are defined in 'Table 1.

Figure 6 Nondimensional stand-off' distance of the external flame versus air/fuel mass ratio at a residual drop radius of 5%. Symbols are defined in 'Table 1.

Figure 7 Fraction of fuel burned during external combustion versus air/fuel mass ratio at a residual drop radius of 5%. Symbols are defined in 'Table 1.

Figure 8 Total fuel fraction burned (flash and external) versus air/fuel mass ratio at a residual drop radius of 5%. Symbols are defined in Table 1.

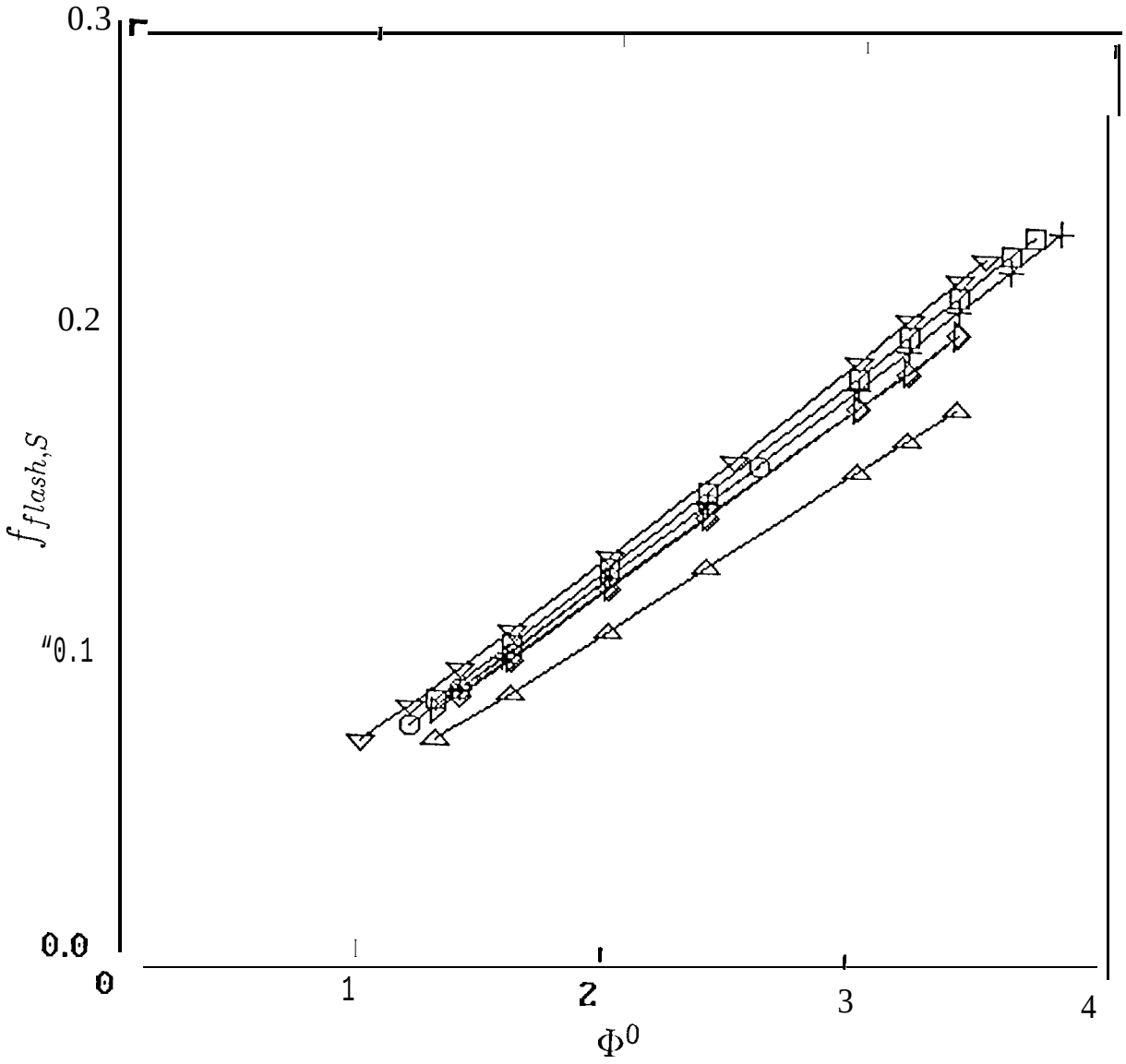

Fig. 1 Bellan

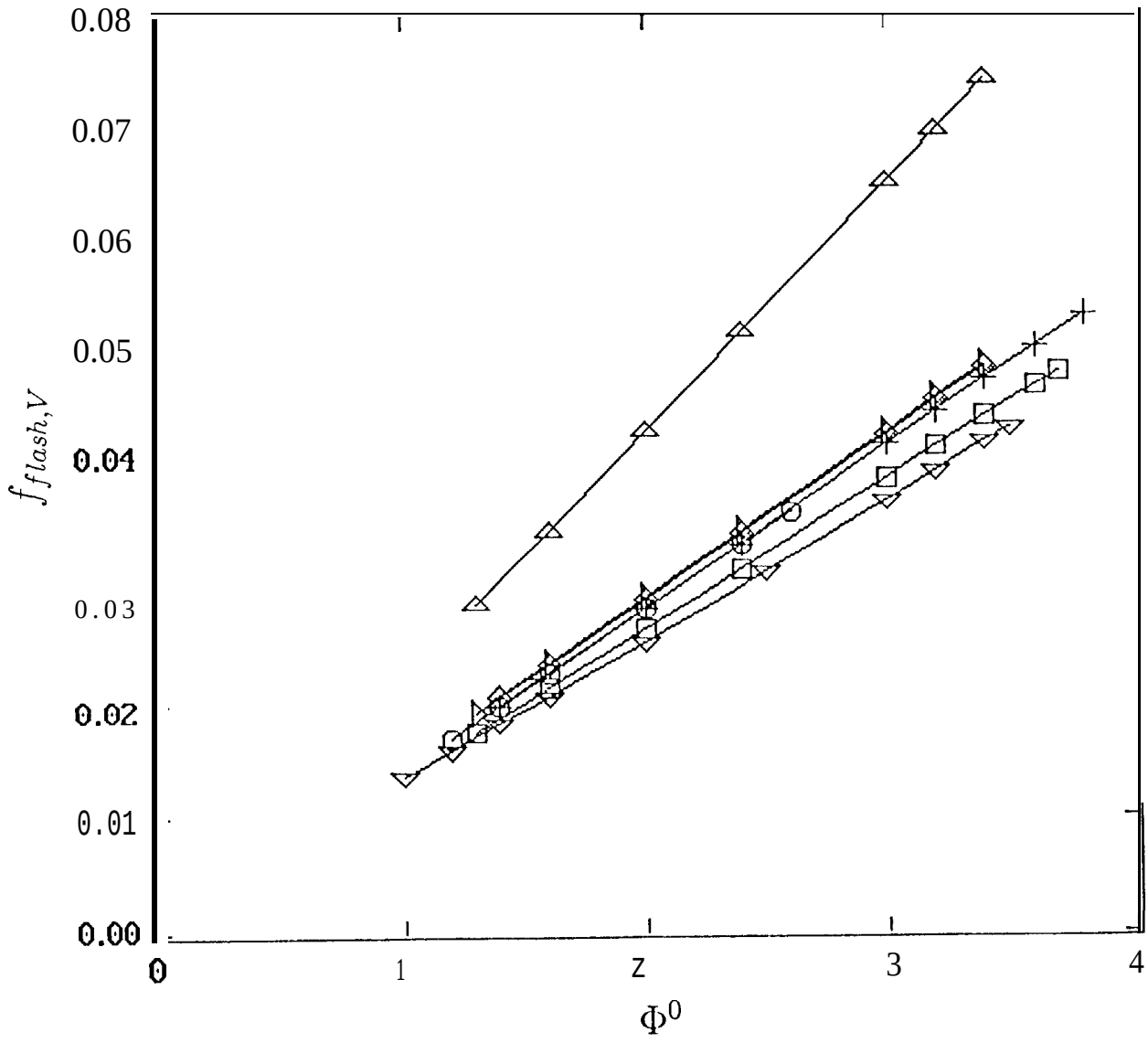

Fig. 2 Bellan

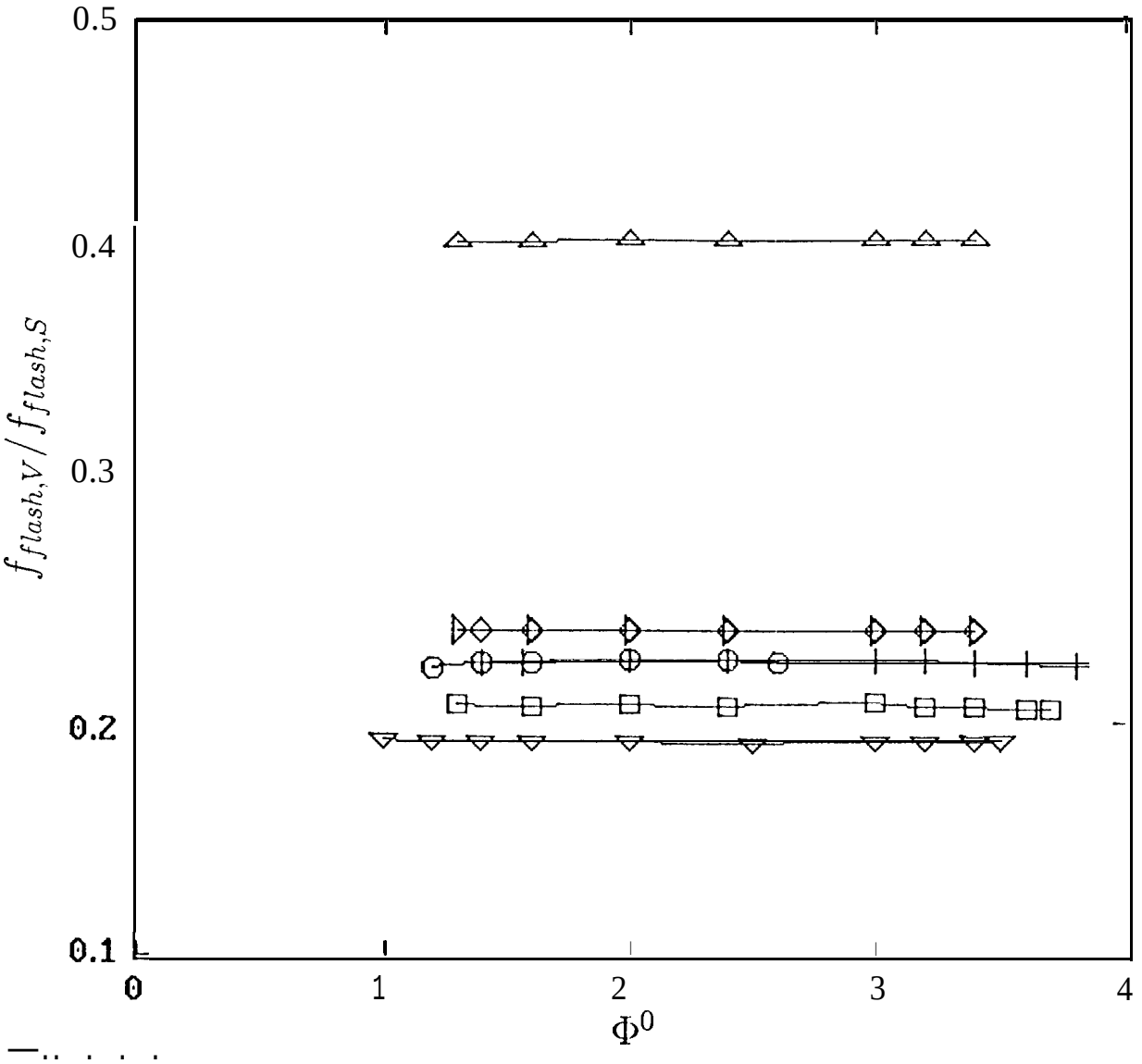

Fig. 3 Bellan

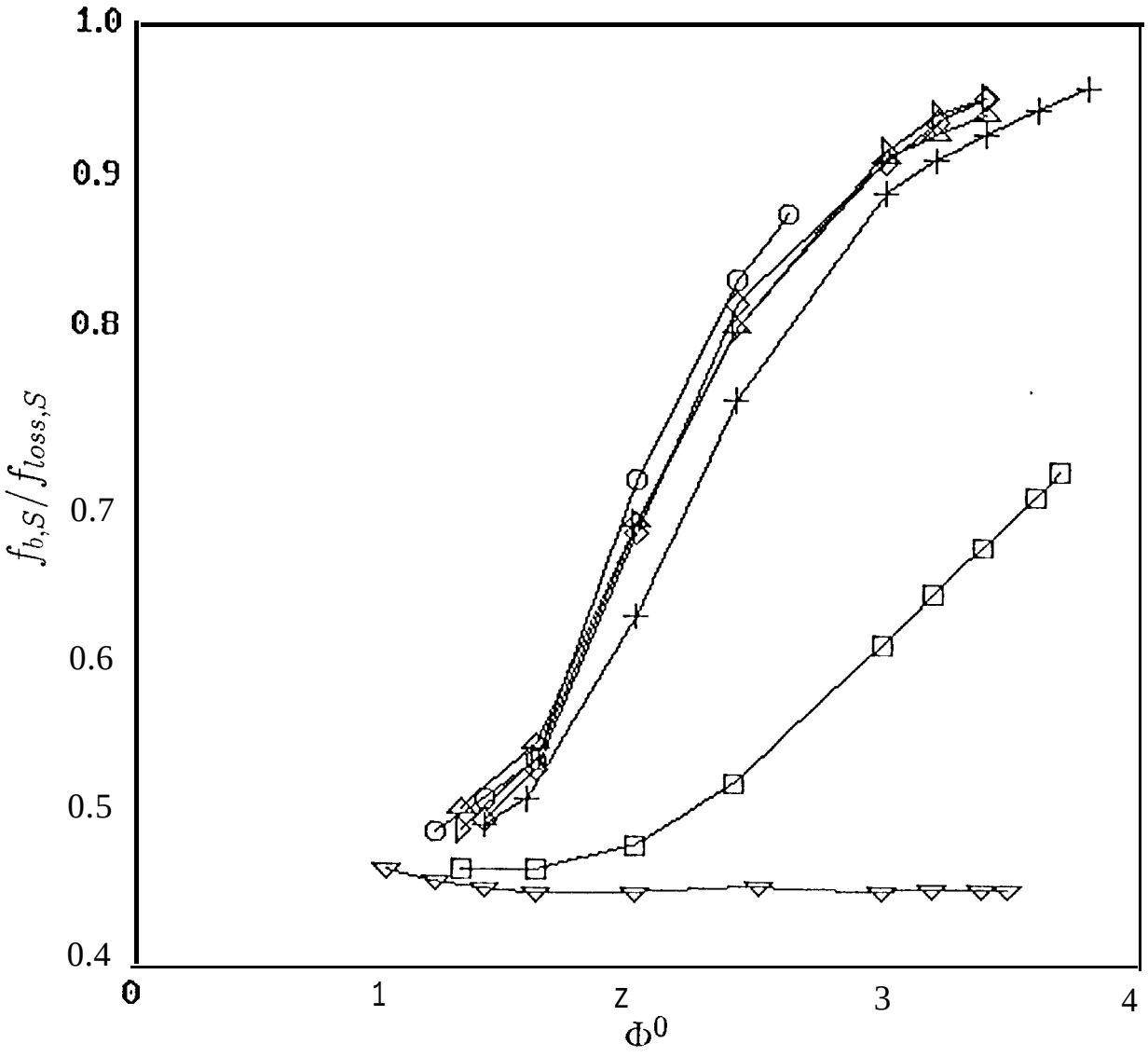

Fig. 4 Bellan

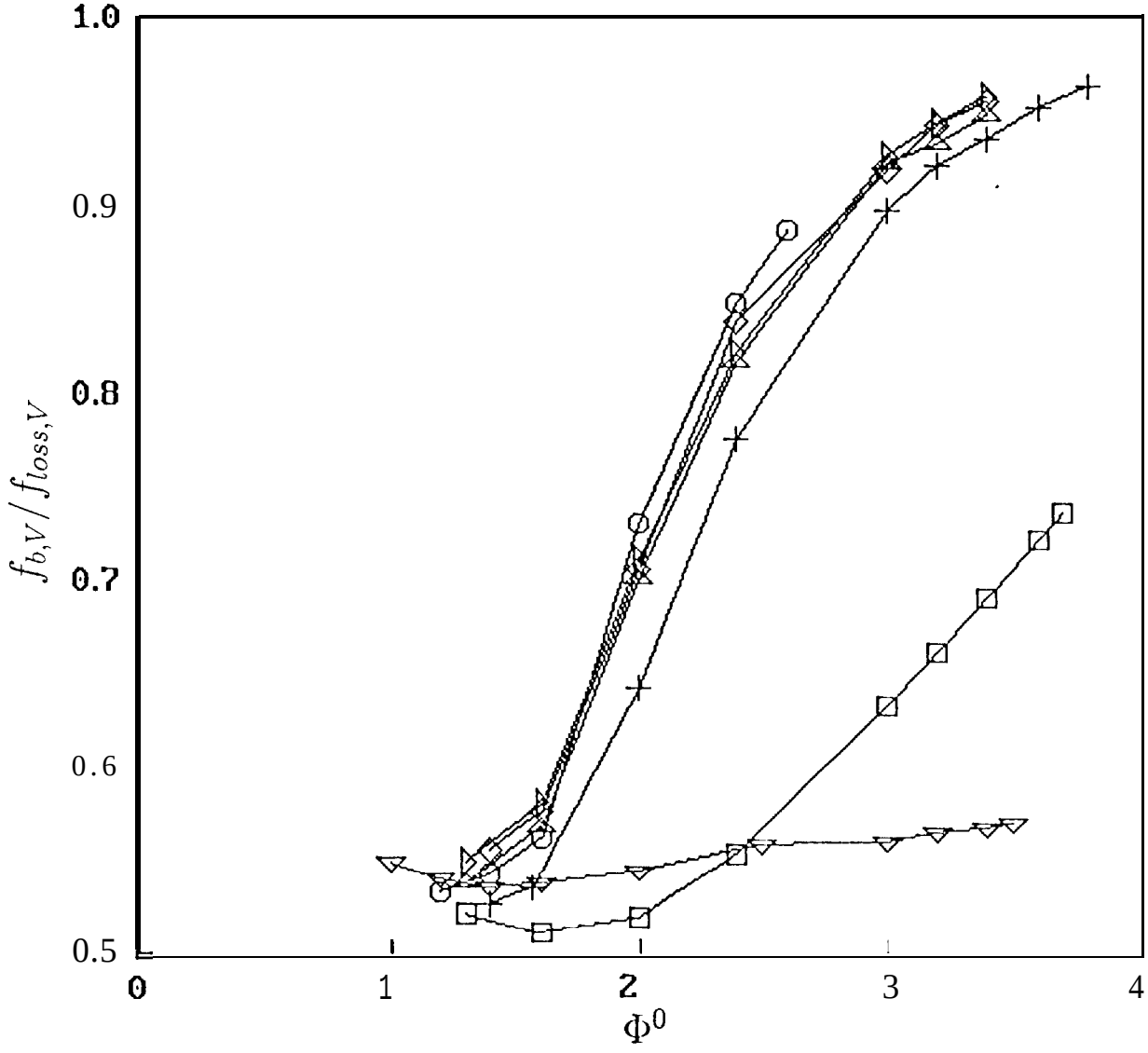

Fig. 5 Bellan

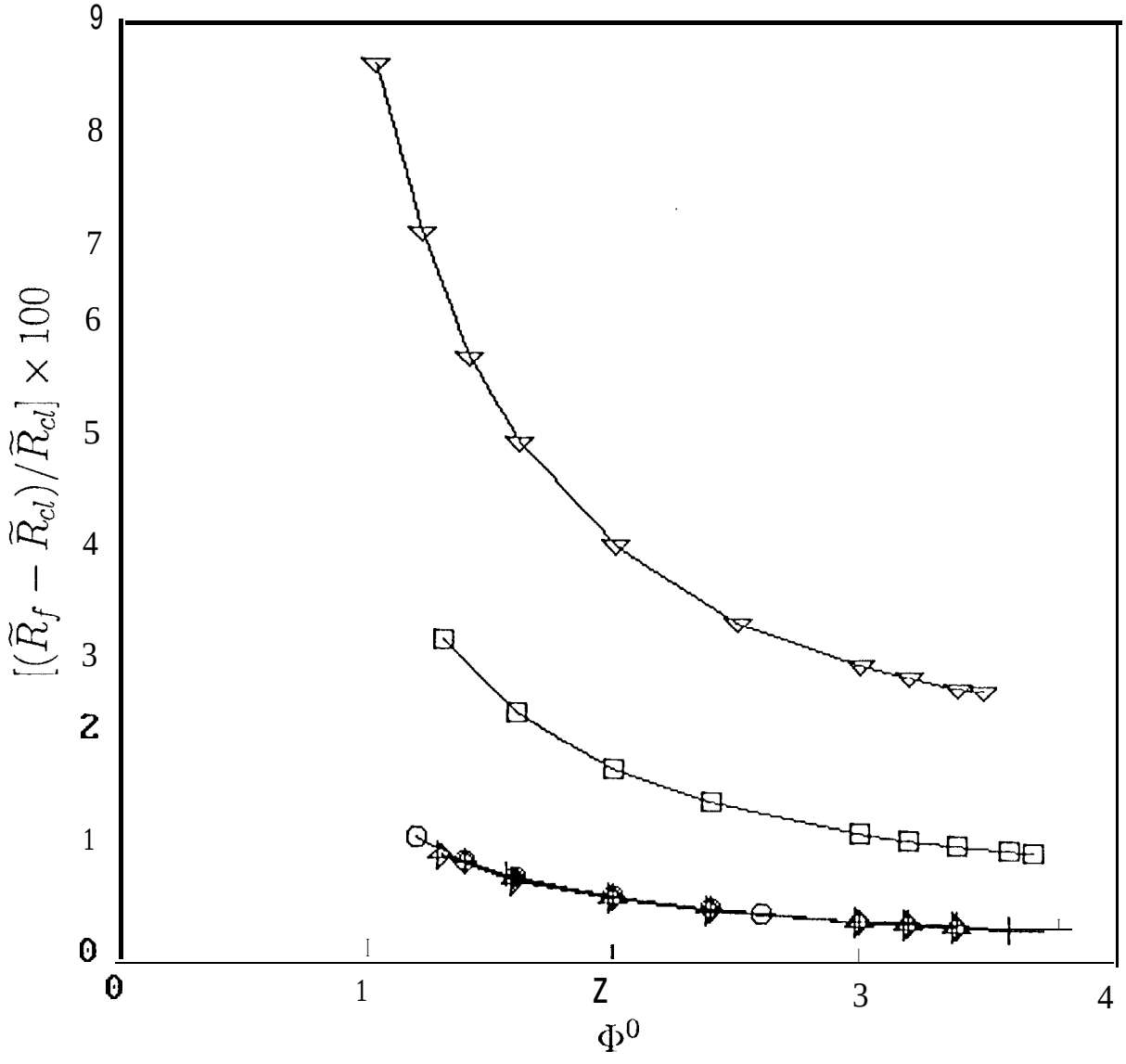
9
8
7
6
5
4
3
2
1
0
0
1
2
3
4
$[(\widetilde{R}_f - \widetilde{R}_{cl})/\widetilde{R}_{cl}] \times 100$
Φ^0

Fig. 6 Bellan

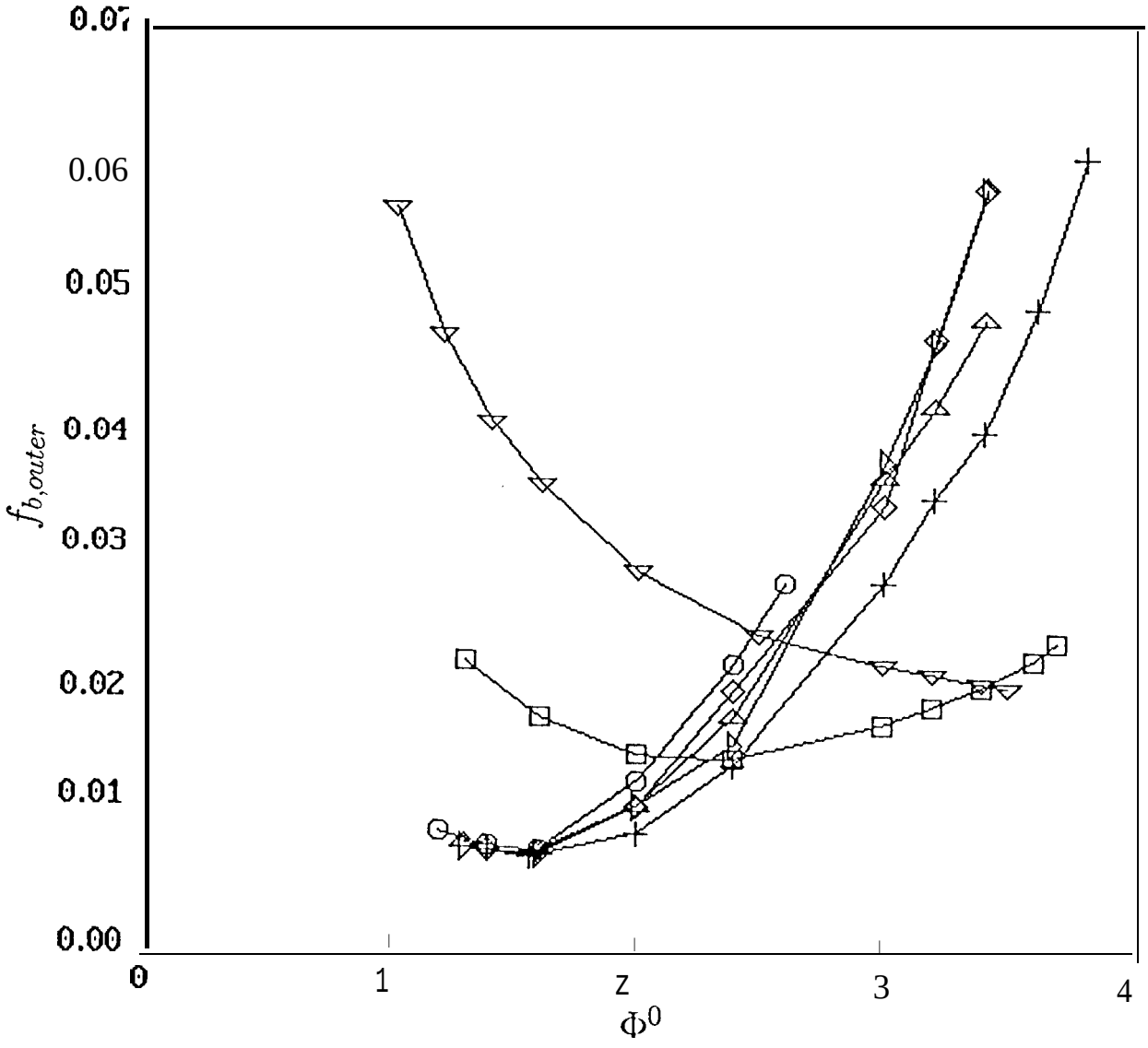

Fig. 7 Ballan

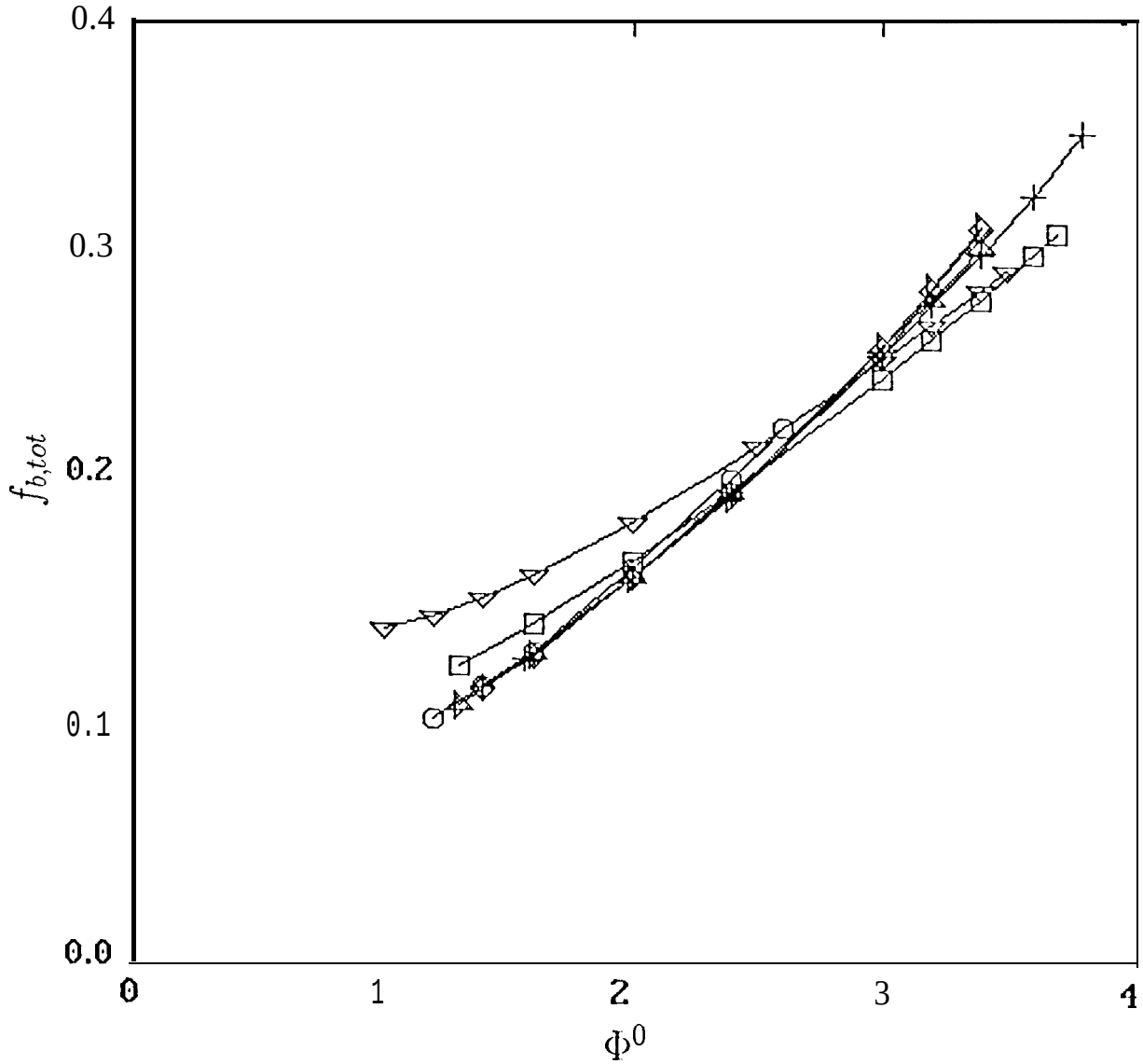

Fig 8. Bellan